

Sign of inverse spin Hall voltages generated by ferromagnetic resonance and temperature gradients in yttrium iron garnet|platinum bilayers

Michael Schreier,^{1,2,*} Gerrit E. W. Bauer,^{3,4,5} Vitaliy I. Vasyuchka,⁶ Joost Flipse,⁷ Ken-ichi Uchida,^{3,8} Johannes Lotze,^{1,2} Viktor Lauer,⁶ Andrii V. Chumak,⁶ Alexander A. Serga,⁶ Shunsuke Daimon,³ Takashi Kikkawa,³ Eiji Saitoh,^{3,4,9,10} Bart J. van Wees,⁷ Burkard Hillebrands,⁶ Rudolf Gross,^{1,11,2} and Sebastian T. B. Goennenwein^{1,11}

¹Walther-Meißner-Institut, Bayerische Akademie der Wissenschaften, Garching, Germany

²Physik-Department, Technische Universität München, Garching, Germany

³Institute for Materials Research, Tohoku University, Sendai, Japan

⁴WPI Advanced Institute for Materials Research, Tohoku University, Sendai, Japan

⁵Kavli Institute of NanoScience, Delft University of Technology, Delft, The Netherlands

⁶Fachbereich Physik and Landesforschungszentrum OPTIMAS,

Technische Universität Kaiserslautern, Kaiserslautern, Germany

⁷Physics of Nanodevices, Zernike Institute for Advanced Materials,
University of Groningen, Groningen, The Netherlands

⁸PRESTO, Japan Science and Technology Agency, Saitama, Japan

⁹Advanced Science Research Center, Japan Atomic Energy Agency, Tokai, Japan

¹⁰CREST, Japan Science and Technology Agency, Tokyo, Japan

¹¹Nanosystems Initiative Munich, Munich, Germany

We carried out a concerted effort to determine the absolute sign of the inverse spin Hall effect voltage generated by spin currents injected into a normal metal. We focus on yttrium iron garnet (YIG)|platinum bilayers at room temperature, generating spin currents by microwaves and temperature gradients. We find consistent results for different samples and measurement setups that agree with theory. We suggest a right-hand-rule to define a positive spin Hall angle corresponding to the voltage expected for the simple case of scattering of free electrons from repulsive Coulomb charges.

The bon mot that the sign is the most difficult concept in physics since there are no approximate methods to determine it has been ascribed to Wolfgang Pauli. Indeed, the struggle to obtain correct signs permeates all of physics. While the negative sign of the electron charge is just a convention, that of derived properties, such as the (conventional) Hall voltage, has real physical meaning. Often it is much easier and sufficient to determine sign differences between related quantities. However, a complete understanding requires not only the relative but also the absolute sign. Here we address the sign of the (inverse) spin Hall effect [(I)SHE] [1–10] and related phenomena. The characteristic parameter is the spin Hall angle, defined as the ratio $\theta_{\text{SH}} \propto J_s/J_c$ of the transverse spin current J_s caused by an applied charge current J_c (a more precise definition is given below). The sign of θ_{SH} may differ for different materials. Since the spin Hall angle for Pt is generally taken to be positive, θ_{SH} of Mo [11], Ta [12], and W [13] must be negative.

The sign of θ_{SH} governs the direction of the spin transfer torque on a magnetic contact relative to that caused by the Oersted magnetic field induced by the same current J_c [12, 13]. It also determines the sign of the induced transverse voltage in experiments in which the ISHE is used to detect spin currents [7]. This technique is now widely used to study spin current injection by a magnetic contact, through “spin pumping” induced by ferromagnetic resonance (FMR) [11, 14–18] or by temperature differences [19–23] (“spin Seebeck effect”, SSE).

However, the pitfalls that can affect the determination of the sign of the θ_{SH} , such as the sign of the spin currents [24] and magnetic field direction are often glossed over in experimental and theoretical papers. Moreover, a mechanism for a sign reversal of the longitudinal spin Seebeck effect has recently been proposed [25]. A careful analysis of experimental results with respect to the signs of FMR and thermal spin pumping voltages generated by the inverse spin Hall effect is therefore overdue.

In this letter we present the results of a concerted action to resolve the sign issue by comparing experiments on microwave-induced spin pumping and spin Seebeck effect for a bilayer of the magnetic insulator yttrium iron garnet (YIG) and platinum (Pt) at room temperature. Samples grown by different techniques have been used in four experimental setups at the Institute for Materials Research, Tohoku University (IMR), Technische Universität Kaiserslautern (UniKL) Zernike Institute for Advanced Materials, University of Groningen (RUG) and the Walther-Meißner-Institut in Garching (WMI). Considering the different sample properties the variations in the magnitude of the observed voltages is not surprising. However, all groups find identical signs for the ISHE Hall voltages that agree with the standard theory for spin pumping by FMR [26] and spin Seebeck effect [27–29]. A positive spin Hall angle can be associated with scattering at negatively charged Coulomb centers in the weakly relativistic electron gas.

Let us define the electron charge as $-e < 0$. We recall that the thumb of the right hand points along the angular momentum $\mathbf{L} = \mathbf{r} \times \mathbf{p}$ of a circulating particle with mass m , position \mathbf{r} and momentum $\mathbf{p} = m\mathbf{v}$

* michael.schreier@wmi.badw.de

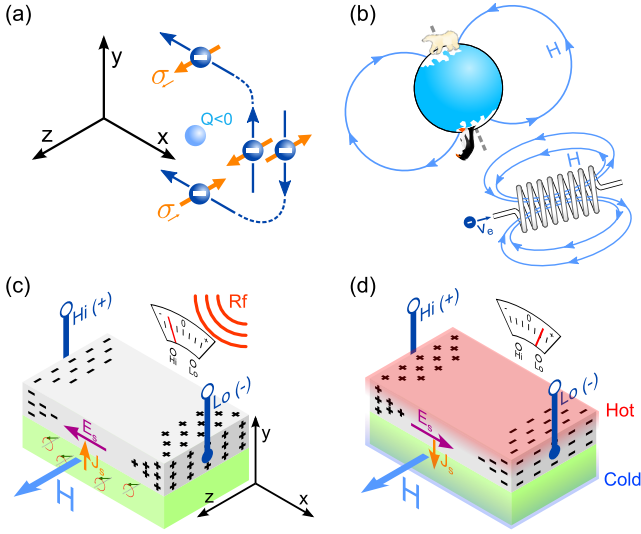


Figure 1. (a) The transverse deflection of polarized electrons generated by a fixed point charge $Q < 0$ that we associate with a positive spin Hall angle. (b) A magnetic field is positive when aligned with the Earth's magnetic field or as the magnetic field generated by a negatively charged particle current flowing through a coil when configured as sketched. [(c),(d)] Typical setups for spin pumping and spin Seebeck experiments, respectively. [(c)] An rf-microwave field excites magnetization precession that relaxes by emitting a spin current into the adjacent Pt layer. [(d)] The spin current from the YIG to the Pt is negative when the latter is hotter. In both cases, the ISHE leads to a voltage between the contacts Hi and Lo .

when the tangential velocity \mathbf{v} is along the fingers of its fist. The magnetic moment of a particle with charge q is given by $\boldsymbol{\mu}_L = q(2m)^{-1}\mathbf{L}$ [30]. This magnetic moment direction is also generated by two monopoles on the \mathbf{L} -axis, the negative (south pole) just below and the positive (north) pole just above the origin. The magnetic moment of the Earth points to the south, so the geographic north pole is actually the magnetic south pole. Hence, the geomagnetic fields on the surface of the Earth as measured by a compass needle point to the north pole. The intrinsic angular momentum (spin) of non-relativistic electrons [31] is $\mathbf{s} = \frac{\hbar}{2}\boldsymbol{\sigma}$, where $\boldsymbol{\sigma}$ is the vector of Pauli spin matrices. The corresponding magnetic moment $\boldsymbol{\mu}_s = -e(2m)^{-1}g\mathbf{s} = -\gamma\mathbf{s}$, where g is the g-factor and γ is the gyromagnetic ratio. In most solids g and therefore γ are positive.

The angular momentum and spin current tensor $\overleftrightarrow{\mathbf{J}}_s$ consists of column vector elements \mathbf{J}_s^α that represent the polarization of angular momentum currents in the Cartesian α -direction, while the row vectors $\mathbf{J}_{s,\beta}$ represent the flow direction of angular momentum along β . The charge- (\mathbf{J}_c) and spin currents are both defined as particle flow (units s^{-1}). We can then define the spin Hall angle θ_{SH} as the proportionality factor in the phenomenological re-

lations

$$\mathbf{J}_{s,\beta} = \theta_{SH}\hat{\beta} \times \mathbf{J}_c \quad (1)$$

$$\mathbf{J}_c = \theta_{SH} \sum_{\alpha} \mathbf{J}_s^{\alpha} \times \hat{\alpha} \quad (2)$$

where the $\hat{\alpha}, \hat{\beta} \in \{\hat{x}, \hat{y}, \hat{z}\}$ are Cartesian unit vectors.

We now demonstrate the physical significance of the sign of θ_{SH} . We do not intend to model the material dependence or contribute to the discussion on whether observed effects are intrinsic or extrinsic. For an external point charge Q at the origin in the weakly relativistic electron gas the bare Coulomb potential at distance r is

$$\phi_0(r) = \frac{1}{4\pi\epsilon_0} \frac{Q}{r}, \quad (3)$$

where ϵ_0 is the vacuum permittivity. In metals $\phi_0(r)$ is screened by the mobile charge carriers to become the Yukawa potential $\phi = \phi_0 e^{-r/\lambda}$. The screening length λ serves to regularize the expectation values, but drops out of the final results. The spin-orbit interaction of an electron in a potential ϕ is equivalent to an effective magnetic field [32]

$$\mathbf{B}_{so} = \frac{-e}{2m^2c^2\gamma} (\nabla\phi \times \mathbf{p}), \quad (4)$$

where c is the velocity of light. The force on the electron then reads

$$\mathbf{F}_{so} = \nabla(\boldsymbol{\mu} \cdot \mathbf{B}_{so}) = \frac{e\hbar}{4m^2c^2} \nabla[\boldsymbol{\sigma} \cdot (\nabla\phi \times \mathbf{p})]. \quad (5)$$

Focussing on a free electron moving in the y -direction ($\mathbf{p} = p_y\hat{y}$) with its spin pointing in the z -direction ($\boldsymbol{\sigma} = \hat{z}\sigma_z$) in an ensemble of randomly distributed identical point with density n , the expectation values $\langle\sigma_z\rangle = 1$ and the average force is

$$\langle\mathbf{F}_{so}^{yz}\rangle = \frac{n}{4\pi\epsilon_0} \frac{4eQ\hbar\pi^2}{3m^2c^2} p_y \hat{x}. \quad (6)$$

For our definition of a positive spin Hall angle we now choose the charge to be negative ($Q < 0$, repulsive). We then arrive at the following right-hand rule: The electron with its spin pointing in the z -direction (thumb) and moving in the y -direction (forefinger) drifts to the negative x -direction (middle finger) [Fig. 1(a)]. A comparison with Eq. (1) and using

$$\mathbf{J}_{s,z} = -\frac{C}{e^2\rho} \nabla\mu_s = \frac{C}{e^2\rho} \langle\mathbf{F}_{so}^{yz}\rangle \quad (7)$$

and

$$\mathbf{J}_c = \frac{p_y}{m} n_e C \hat{y} \quad (8)$$

where μ_s is the spin chemical potential, ρ is the resistivity, C is the cross sectional area the currents are flowing

through, and n_e is the carrier density, leads to a spin Hall angle

$$\theta_{\text{SH}} = -\frac{n}{4\pi\epsilon_0} \frac{4eQ\hbar\pi^2}{3m^2c^2} \frac{m}{e^2\rho n_e}. \quad (9)$$

Inserting numbers for fundamental constants $\theta_{\text{SH}} \cong \pm 3 \times 10^{-10} \Omega\text{m} \times n/(n_e\rho)$ for $Q = \mp e$.

The time-averaged spin current injected by a steady precession [26] around the equilibrium magnetization with unit vector $\hat{\mathbf{m}}$ is polarized along $\hat{\mathbf{m}}$. This spin pumping process is associated with energy relaxation of the magnetization dynamics that increases the magnetic moment in the direction of the effective magnetic field. When the g -factor is positive, the spin pumping current through the interface is positive as well. In the SSE, when the temperature of the magnetization is *lower* than that of the electrons in the metal, the energy and, if $g > 0$, spin current is opposite to that under FMR [27], leading to an opposite sign in the ISHE voltage compared to the FMR. Under open circuit conditions the inverse spin Hall effect [Eq. (2)] leads to a charge separation and an electrostatic field

$$\mathbf{E}_s = \frac{-e\rho}{A} \theta_{\text{SH}} [\mathbf{J}_{s,\hat{\mathbf{m}}} \times \hat{\mathbf{m}}], \quad (10)$$

where A is the area of the ferromagnet|metal interface and ρ is the resistivity of the metal layer. This corresponds to an electromotive force $\mathcal{E} = -\mathbf{E}_s \cdot \mathbf{l}$, where \mathbf{l} is the length vector from the *Lo* to the *Hi* contact in Fig. 1(c) and (d).

The sign of an applied magnetic field is related to the current direction according to Ampere's right hand law as depicted in Fig. 1(b). In practice, it is convenient to use a compass needle for comparison with the Earth's magnetic field. Fig. 1(b) defines the positive field direction from the antarctic to the arctic, i.e. along the geomagnetic field. Typical experimental setups for spin pumping [(c)] and spin Seebeck experiments [(d)] on yttrium iron garnet|platinum thin film (YIG|Pt) bilayers are also sketched in Fig. 1. In the former, a ferromagnet (F)|normal metal (N) stack is exposed to microwave radiation with frequency f (typically in the GHz regime), while in spin Seebeck experiments the bilayer is exposed to a thermal gradient. Sample parameters used by the different groups are listed in the third column of Fig. 2. For details on the sample fabrication we refer to Refs. 33 and 34 (WMI), Ref. 18 (RUG), Refs. 35 and 36 (UniKL) and Ref. 37 (IMR).

Fig. 2 summarizes the results of the participating groups. Note that in each group both the spin pumping and spin Seebeck experiments were performed on the same sample, without changing the setup.

At the WMI, FMR experiments (first row) were carried out in a microwave cavity with fixed frequency $f_{\text{res}} = 9.82 \text{ GHz}$ as a function of an applied magnetic field H_{ext} leading to resonance at $\mu_0 H_{\text{ext}} \cong 270 \text{ mT}$. A source meter was used to drive a large ($I_h = \pm 20 \text{ mA}$) dc

charge current through the platinum film ($R_{\text{Pt}} = 197 \Omega$) in order to generate a temperature gradient (hot Pt, cold YIG) [23]. By summing voltages recorded for opposite I_h directions, the magnetoresistive contributions cancel out, such that only the spin Seebeck signal remains. The ISHE voltages for both FMR and the spin Seebeck experiments were measured by the same, identically connected nanovoltmeter with microwave and heating current separately turned on.

Results from the UniKL are shown in the second row in Fig. 2. A microwave with $f_{\text{res}} = 7 \text{ GHz}$ fed into a Cu stripline on top of the Pt film excites the FMR at an external magnetic field of $\mu_0 H_{\text{ext}} \cong 175 \text{ mT}$. The microwave current amplitude was modulated at a frequency of $f_{\text{mod}} = 500 \text{ Hz}$ to allow for lock-in detection of the induced voltages [36] that are measured by a nanovoltmeter. The spin pumping data show a small offset between positive and negative magnetic fields, which stems from Joule heating in the Pt layer by the microwaves. Peltier elements on the top and bottom (separated by an AlN layer) generated a thermal gradient for the spin Seebeck experiments that were reversed for cross checks, as shown in the right graph.

The third row in Fig. 2 shows the results obtained at the IMR. Here, the sample is placed on a coplanar waveguide such that at $f_{\text{res}} = 3.8 \text{ GHz}$ FMR condition is fulfilled for $\mu_0 H_{\text{ext}} \cong 70 \text{ mT}$. The thermal gradient for the spin Seebeck measurements was generated by an electrically isolated separate heater on top of the Pt.

The fourth row in Fig. 2 shows the RUG results. A coplanar waveguide on top of the YIG was used to excite the FMR at a magnetic field of $\mu_0 H_{\text{ext}} \cong 6 \text{ mT}$. The spin Seebeck effect was detected using an ac-variant of the current heating scheme. The spin Seebeck voltage can thereby be detected as described above in the second harmonic of the ac voltage signal.

In spite of differences in samples and measurement techniques, all experiments agree on the sign for spin pumping and spin Seebeck effect. We all measure *negative* spin pumping and *positive* spin Seebeck voltages for positive applied magnetic fields that all change sign when the magnetic field is reversed, consistent with the theoretical expectations [1, 2, 26, 27].

We can now address the *absolute* sign of the spin Hall angle. The results in Fig. 2 were obtained with measurement configurations equivalent to the one depicted in Figs. 1(c) and (d). With external magnetic field \mathbf{H}_{ext} pointing in the $\hat{\mathbf{z}}$ direction $\hat{\mathbf{m}} = \hat{\mathbf{z}}$ and $\hat{\mathbf{J}}_s = \hat{\mathbf{y}}$ for FMR spin pumping. According to Eq. (10), when $\theta_{\text{SH}} > 0$ $\mathbf{E}_s = -\hat{\mathbf{x}}$, which leads to a negative (positive) charge accumulation at the $-x$ ($+x$) edge of the Pt film and a negative spin pumping voltage is expected as well as observed. In the spin Seebeck experiments with Pt hotter than YIG, the spin current flows in the opposite direction ($\hat{\mathbf{J}}_s = -\hat{\mathbf{y}}$), and the voltage is inverted. Therefore, the spin Hall angle of Pt is positive if defined as above. The nature of the spin Hall effect in Pt is likely to be governed by its electronic band

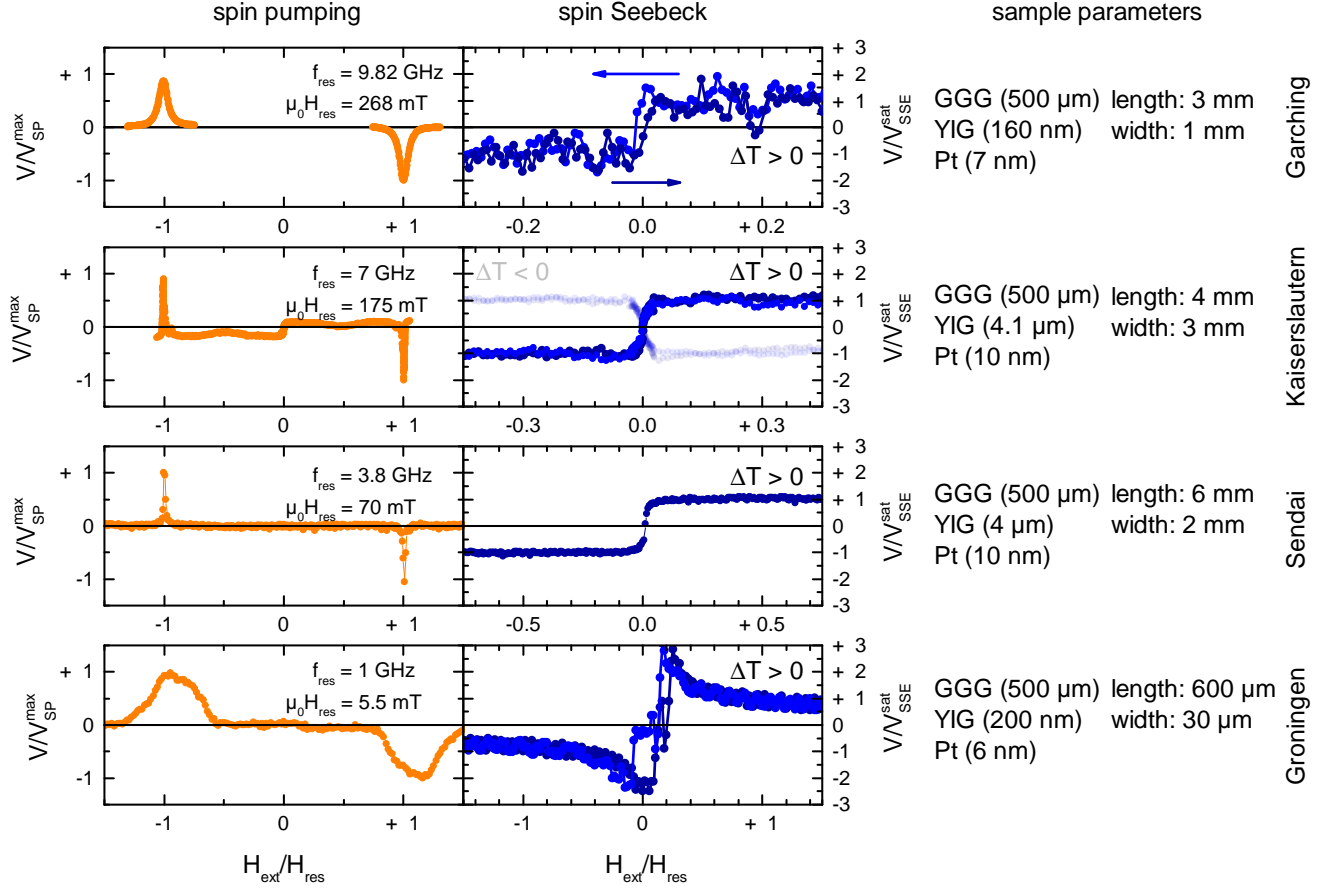


Figure 2. Measured voltage signals for the FMR spin pumping (left column) and spin Seebeck (middle column) experiments obtained by the contributing groups. The voltage signals have been normalized to a maximum modulus of unity while the applied magnetic fields are in units of the FMR resonance field H_{res} given in the insets. The temperature difference $\Delta T = T_{\text{Pt}} - T_{\text{YIG}}$ is positive. The third column lists sample layer thicknesses and dimensions. The sign of the observed voltages is consistent between the individual groups.

structure [38], but it should be helpful to know that the sign is identical to that caused by negatively charged impurities.

In summary, we present spin pumping and spin Seebeck experiments for various samples and experimental conditions leading to gratifying agreement of the results obtained by different groups. By carefully accounting for the signs of all experimental parameters and definitions we were able to determine both the relative and the absolute signs of both effects, linking the positive spin Hall angle of Pt to a simple physical model of negative scattering centers. The relative signs of spin pumping and spin Seebeck effect are consistent with theoretical predictions [14, 27–29]. The techniques and samples

used in this letter are representative for a large number of spin pumping and spin Seebeck experiments and should serve as a reference for other materials or sample geometries.

We thank M. Wagner, M. Althammer and M. Opel for sample preparation and gratefully acknowledge financial support by the DFG via SPP 1538 “Spin Caloric Transport” (projects GO 944/4-1, SE 1771/4-1, BA 2954/1-1) and CH 1037/1-1, NanoLab NL and the Foundation for Fundamental Research on Matter (FOM), JSPS Grants-in-Aid for Scientific Research, EU-RTN Spinicur, EU-FET InSpin 612759, PRESTO-JST “Phase Interfaces for Highly Efficient Energy Utilization”, and CREST-JST “Creation of Nanosystems with Novel Functions through Process Integration”.

[1] M. I. D’yakonov and V. I. Perel’, JETP Lett. **13**, 467 (1971).

[2] J. E. Hirsch, Phys. Rev. Lett. **83**, 1834 (1999).

- [3] S. Zhang, Phys. Rev. Lett. **85**, 393 (2000).
- [4] S. Murakami, in *Advances in Solid State Physics*, Advances in Solid State Physics, Vol. 45, edited by B. Kramer (Springer Berlin Heidelberg, 2006) pp. 197–209.
- [5] J. Sinova, D. Culcer, Q. Niu, N. A. Sinitsyn, T. Jungwirth, and A. H. MacDonald, Phys. Rev. Lett. **92**, 126603 (2004).
- [6] Y. K. Kato, R. C. Myers, A. C. Gossard, and D. D. Awschalom, Science **306**, 1910 (2004).
- [7] E. Saitoh, M. Ueda, H. Miyajima, and G. Tatara, Appl. Phys. Lett. **88**, 182509 (2006).
- [8] S. O. Valenzuela and M. Tinkham, Nature **442**, 176 (2006).
- [9] T. Kimura, Y. Otani, T. Sato, S. Takahashi, and S. Maekawa, Phys. Rev. Lett. **98**, 156601 (2007).
- [10] J. Wunderlich, B.-G. Park, A. C. Irvine, L. P. Zrbo, E. Rozkotov, P. Nemec, V. Novk, J. Sinova, and T. Jungwirth, Science **330**, 1801 (2010).
- [11] O. Mosendz, V. Vlaminck, J. E. Pearson, F. Y. Fradin, G. E. W. Bauer, S. D. Bader, and A. Hoffmann, Phys. Rev. B **82**, 214403 (2010).
- [12] L. Liu, C.-F. Pai, Y. Li, H. W. Tseng, D. C. Ralph, and R. A. Buhrman, Science **336**, 555 (2012).
- [13] C.-F. Pai, L. Liu, Y. Li, H. Tseng, D. Ralph, and R. Buhrman, Appl. Phys. Lett. **101**, 122404 (2012).
- [14] Y. Tserkovnyak, A. Brataas, and G. E. W. Bauer, Phys. Rev. B **66**, 224403 (2002).
- [15] K. Ando, Y. Kajiwara, K. Sasage, K. Uchida, and E. Saitoh, IEEE Trans. Magn. **46**, 3694 (2010).
- [16] C. W. Sandweg, Y. Kajiwara, A. V. Chumak, A. A. Serga, V. I. Vasyuchka, M. B. Jungfleisch, E. Saitoh, and B. Hillebrands, Phys. Rev. Lett. **106**, 216601 (2011).
- [17] F. D. Czeschka, L. Dreher, M. S. Brandt, M. Weiler, M. Althammer, I.-M. Imort, G. Reiss, A. Thomas, W. Schoch, W. Limmer, H. Huebl, R. Gross, and S. T. B. Goennenwein, Phys. Rev. Lett. **107**, 046601 (2011).
- [18] V. Castel, N. Vlietstra, J. Ben Youssef, and B. J. van Wees, Appl. Phys. Lett. **101**, 132414 (2012).
- [19] K. Uchida, S. Takahashi, K. Harii, J. Ieda, W. Koshibae, K. Ando, S. Maekawa, and E. Saitoh, Nature **455**, 778 (2008).
- [20] K. Uchida, H. Adachi, T. Ota, H. Nakayama, S. Maekawa, and E. Saitoh, Appl. Phys. Lett. **97**, 172505 (2010).
- [21] C. M. Jaworski, J. Yang, S. Mack, D. D. Awschalom, J. P. Heremans, and R. C. Myers, Nat Mater **9**, 898 (2010).
- [22] D. Qu, S. Y. Huang, J. Hu, R. Wu, and C. L. Chien, Phys. Rev. Lett. **110**, 067206 (2013).
- [23] M. Schreier, N. Roschewsky, E. Dobler, S. Meyer, H. Huebl, R. Gross, and S. T. B. Goennenwein, Appl. Phys. Lett. **103**, 242404 (2013).
- [24] B. Jonker, A. Hanbicki, D. Pierce, and M. Stiles, J. Magn. Magn. Mater. **277**, 24 (2004).
- [25] H. Adachi, K. Uchida, E. Saitoh, and S. Maekawa, Rep. Prog. Phys. **76**, 036501 (2013).
- [26] Y. Tserkovnyak, A. Brataas, and G. E. W. Bauer, Phys. Rev. Lett. **88**, 117601 (2002).
- [27] J. Xiao, G. E. W. Bauer, K. Uchida, E. Saitoh, and S. Maekawa, Phys. Rev. B **81**, 214418 (2010).
- [28] H. Adachi, J.-i. Ohe, S. Takahashi, and S. Maekawa, Phys. Rev. B **83**, 094410 (2011).
- [29] S. Hoffman, K. Sato, and Y. Tserkovnyak, Phys. Rev. B **88**, 064408 (2013).
- [30] J. Jackson, *Classical electrodynamics* (Wiley, 1975).
- [31] L. I. Schiff, *Quantum Mechanics* (McGraw-Hill, 1949).
- [32] H.-A. Engel, E. I. Rashba, and B. I. Halperin, “Theory of spin hall effects in semiconductors,” in *Handbook of Magnetism and Advanced Magnetic Materials* (John Wiley & Sons, Ltd, 2007).
- [33] S. Geprägs, S. Meyer, S. Altmannshofer, M. Opel, F. Wilhelm, A. Rogalev, R. Gross, and S. T. B. Goennenwein, Appl. Phys. Lett. **101**, 262407 (2012).
- [34] M. Althammer, S. Meyer, H. Nakayama, M. Schreier, S. Altmannshofer, M. Weiler, H. Huebl, S. Geprägs, M. Opel, R. Gross, D. Meier, C. Klewe, T. Kuschel, J.-M. Schmalhorst, G. Reiss, L. Shen, A. Gupta, Y.-T. Chen, G. E. W. Bauer, E. Saitoh, and S. T. B. Goennenwein, Phys. Rev. B **87**, 224401 (2013).
- [35] M. B. Jungfleisch, T. An, K. Ando, Y. Kajiwara, K. Uchida, V. I. Vasyuchka, A. V. Chumak, A. A. Serga, E. Saitoh, and B. Hillebrands, Appl. Phys. Lett. **102**, 062417 (2013).
- [36] M. B. Jungfleisch, V. Lauer, R. Neb, A. V. Chumak, and B. Hillebrands, Appl. Phys. Lett. **103**, 022411 (2013).
- [37] Z. Qiu, K. Ando, K. Uchida, Y. Kajiwara, R. Takahashi, H. Nakayama, T. An, Y. Fujikawa, and E. Saitoh, Appl. Phys. Lett. **103**, 092404 (2013).
- [38] G. Y. Guo, S. Murakami, T.-W. Chen, and N. Nagaosa, Phys. Rev. Lett. **100**, 096401 (2008).